Results in Physics 13 (2019) 102211

Contents lists available at ScienceDirect

Results in Physics

journal homepage: www.elsevier.com/locate/rinp

Review of recent gamma spectrum unfolding algorithms and their application

Fei Li[a,b,*], Zhixing Gu[a,b], Liangquan Ge[b], Hui Li[b], Xinyu Tang[b], Xinle Lang[b], Bo Hu[b]

[a] Applied Nuclear Technology in Geosciences Key Laboratory of Sichuan Province, Chengdu University of Technology, China
[b] College of Nuclear Technology and Automation Engineering, Chengdu University of Technology, China

ARTICLE INFO

Keywords:
Gamma spectrum
Unfolding algorithm
Denoising
Background subtraction
Overlapping peak separation

ABSTRACT

Gamma spectrum analysis is regarded as a fast, reliable and non-destructive technology on determining the type and intensity of radionuclides. It is widely used in nuclear physics research, geological exploration, environmental assessment. Under the certain condition (detector, electronic components and measuring environment), the data obtained by different unfolding algorithms have different results. The accuracy of qualitative and quantitative analysis of radionuclides is determined by gamma spectrum unfolding technique. This paper mainly analyzes the development and application of the gamma spectrum unfolding algorithms and technologies in denoising, background subtraction and overlapping peak separation, reviews the performances, results and highlights of the typical algorithms, discusses representative examples and proposes potential research directions.

Introduction

Gamma spectrometry is based on the physical mechanism of the interaction between gamma rays and target matter. In the process of gamma spectrometry, the signals are obtained and converted to measurable and recordable electrical pulse signals through the electronic components. With multi-channel pulse analyzer, the type of the nuclide can be identified according to the electrical pulse peak (energy), the concentration of the nuclide can be calculated by counting (intensity) [1]. Gamma spectrometry can be divided into ground gamma survey and aerial gamma survey on the basis of measuring object [2], and the method is widely used in the fields of environmental radiation monitoring, radioactive mineral exploration, radiation therapy, food hygiene inspection, etc. [3–6].

The most common used gamma spectrometers for radionuclide measurement on market are high-purity germanium (HPGe) gamma spectrometer, $LaBr_3$ gamma spectrometer and NaI (Tl) gamma spectrometer according to the reviewed work. HPGe detector is the nuclear radiation detector made from high purity germanium crystals, it has high energy resolution that can reach 2.0 keV at 1332 keV of ^{60}Co. For complex gamma-ray energy input, HPGe detector has strong resolving power, but its working temperature has to be set as low as the liquid nitrogen temperature. Furthermore, HPGe detector has low detection efficiency and costs high that causes the conditions of use would be affected by certain restrictions [7]. $LaBr_3$ is a new scintillation detector, which has attracted much attention in recent years. Its energy resolution is about 3% at 661 keV of ^{137}Cs. The detection efficiency of $LaBr_3$ is significantly improved while the large-size process technology is getting advance, but the large-size detector is expensive in construction [8]. The energy resolution of NaI (Tl) detector is relatively low. At 661 keV of ^{137}Cs, the energy resolution is generally about 8%. If the multi-nuclide sample is measured under the high background measurement environment, the spectrum component would be fairly complex. However, NaI (Tl) gamma spectrometer is widely used in practical monitoring because of its high detection efficiency and low cost [9].

In general, due to the influence of different instrument electronic components, temperature, humidity and other factors, the spectrum presented is relatively different. In the case of low energy resolution, complex and accurate gamma spectrum unfolding algorithm is needed to perform spectral analysis effectively and reliably [10]. The main gamma spectrum unfolding tasks include spectral data smoothing (denoising), background subtraction, peak searching (overlapping peak separation), peak area calculation and nuclide content calculation. Due to the statistical fluctuation influence measurement, noisy electronic circuits, gamma ray scattering, the situation of statistical fluctuation of measured gamma spectrum has an inevitable influence on the analysis of the gamma spectrum unfolding. At the same time, background interference can cause the peak area calculation and weak peak flood, in order to directly affect the accuracy of the gamma spectrum data analysis [11]. In terms of gamma spectrum unfolding, the spectrum

* Corresponding author at: Applied Nuclear Technology in Geosciences Key Laboratory of Sichuan Province, Chengdu University of Technology, China.
E-mail address: lifeimvp@sina.com (F. Li).

https://doi.org/10.1016/j.rinp.2019.102211
Received 4 December 2018; Received in revised form 3 March 2019; Accepted 17 March 2019
Available online 21 March 2019

smoothing, background subtraction and overlapping peak separation is the most difficult aspect and the most studied direction. Common spectrum smoothing methods include exponential smoothing, Markov smoothing, Fourier transform, wavelet transform, etc. [12–15]. Background subtraction generally includes linear method, phase step background subtraction, SNIP method, Fourier transform method, etc. [16–19]. The overlapping peak separation mainly consists of function fitting method, deconvolution method, and wavelet transform method [20–22]. For the same complex gamma spectrum data, selecting different spectral algorithms can obtain different analytical results. Therefore, optimization and design of more accurate and precise gamma spectrum unfolding algorithm are the development trend and emphasis of the research in the field of gamma spectrum data processing [23].

This paper describes and comments on the development of the gamma spectrum unfolding algorithm in spectra denoising, background subtraction and overlapping peak separation. It is impossible to analyze all relevant literatures because of personal limitation. Therefore, our focus is on the representative technology or application, to review the development status of the algorithm, and to analyze the advantages and disadvantages of the application, so as to provide a more accurate and effective reference for the researchers of gamma spectrum unfolding technology.

Spectra denoising

Due to the decay of the nucleus, statistical fluctuations inherent in the detection instrument and the influence of the noise of the electronic system in the measured gamma spectrum, it is inevitable that the measured spectral data would be greatly influenced by statistical fluctuations and interference noise [24,25]. This phenomenon leads to errors in the process of the gamma spectrum analysis, which is unfavorable for searching the characteristic spectrum and subsequent spectrum analysis. Therefore, the spectrum needs to be smoothed and denoised before qualitative and quantitative analysis [26].

Generally, the denoising effect is evaluated from smoothness index and similarity. The smoothness index is expressed by the ratio of the spectral data of the noise reduction to the variance of the difference of the original data, and is denoted as r, which is inversely proportional to the denoising effect. In many of the current studies, the most commonly used criterion for judging the denoising effect is the root mean square error (RMSE), which is inversely proportional to the similarity [27–31].

The purpose of denoising (data smoothing) is to eliminate statistical fluctuations when data characteristics are as small as possible, and to conduct early processing or calculate peak area for quantitative analysis before searching peak. Data smoothing would decrease peak height, increase peak width, and cause a negative effect on smoothness [32,33].

The de-noising method of gamma spectrum can be roughly divided into two categories: finite impulse response (FIR) convolution filtering and wavelet decomposition de-noising. Both of them use a group of basis functions to fit the spectrum data, but the specific processing mode is different. The former adopts the polynomial and the Gaussian function basis, and carries on the local fitting approximation to the data through the least square principle, such as the Gaussian denoising method [34], the gravity method [35], the least square method [36], etc. The latter adopts the wavelet basis, uses the group of high-pass and low-pass filter to perform multistage decomposition of data, reconstructs the coefficients after the threshold decomposition, and obtains the fitting approximation of the original data. Basically, it is a time-frequency analytical de-noising concept [37]. Common methods are wavelet transform [38], Fourier transform [39], noise adjusted singular value decomposition (NASVD) [40], etc.

The least square method

The least square method was first proposed by Adrien-Marie Legendre. It is a mathematical optimization procedure for finding the best-fitting curve. When a set of points are given, it can fit a curve by minimizing the sum of the squares [41–44].

In 2013, in order to solve the problem that the linear smoothing method may lose the characteristic peak of important radionuclides during processing, Sida Sun et al. proposed an adaptive smoothing method to improve the accuracy of gamma spectrum [45]. The result of this method was compared with the peak height and full width at half maxima (FWHM) obtained by the original data and three-point smoothing method. It showed that the peak height was only slightly reduced. Peak shape was accurately maintained without the amplification effect. This method effectively reduced the statistical fluctuation of gamma ray spectrum measurement while greatly maintaining the weak peak. It can greatly improve peak identification and the accuracy of peak calculation.

In 2014, with the purpose of avoiding setting weights, Yang Xiaowei et al. proposed a robust least squares support vector machine (RLS-SVM) based on the stage least squares loss function, and proposed continuously improved method based on an iterative algorithm based on the concave-convex process and Newton [46]. The method can overcome the problem of the outlier or noise sensitivity of the least squares support vector machine in the data setting.

Wang Qin et al. proposed the basic idea of least squares curve fitting in 2015 [47]. The fitting curve of least squares can be obtained by minimizing the sum of squares of all data points and the error of the estimated point or fitting point. The fitting function of the least square method is described by the formula:

$$f_k(x_i) = \sum_{k=0}^{n} a_k x_i^k, \begin{cases} k = 1 \\ k > 1 \end{cases}$$

This formula is one of the most commonly used curve fitting algorithm, where a_k (k = 0, 1, 2… n) is the only solution to the equation.

In 2017, Liu Jun et al. considered the previous studies and proposed the least squares support vector machine (LS-SVW) spectrum denoising method based on the least square method [48]. In this method, the spectrum was segmented according to the principle of three-window method. The weighted stacking smoothing was performed at the breakpoint of the segmentation to avoid excessive changes in the first derivative at the segmentation point.

$$\mathrm{Y(i)} = \begin{cases} y_1(i); & 1 \le i < 34 - t \\ y_2(i); & 34 + t < i < 114 - t \\ y_3(i); & 114 + t < i < 256 \\ k_j \cdot y_1(i) + \bar{k_j} \cdot y_2(i); & 34 - t \le i \le 34 + t \\ k_j \cdot y_2(i) + \bar{k_j} \cdot y_3(i); & 114 - t \le i \le 114 + t \end{cases}$$

where i is the spectrum channel, y_1, y_2, and y_3 are the results of spectrum three-section regression fitting, and the channel distribution of the three-energy segment is (1 ~ 34 + t), (34 − t ~ 114 + t), and (114 − t ~ 256), respectively. The overlapping channel address of the spectrum is 2 t + 1. k_j and —k—k_j are the smoothing weighting factors and their mathematical expressions are described in formulas:

$$k_j = \frac{1}{2} + \frac{1}{2}\sin\left(\frac{j-1}{2t}\pi + \frac{\pi}{2}\right) j = 1, 2, \cdots, 2t + 1$$

$$\bar{k_j} = \frac{1}{2} - \frac{1}{2}\sin\left(\frac{j-1}{2t}\pi + \frac{\pi}{2}\right) j = 1, 2, \cdots, 2t + 1$$

where j states the position number of the sampled data in the overlapped data segment.

The results showed that the method can preserve the most spectrum information while eliminating noise. The smoothing results had the advantages of uniqueness, strong adaptability and generalization.

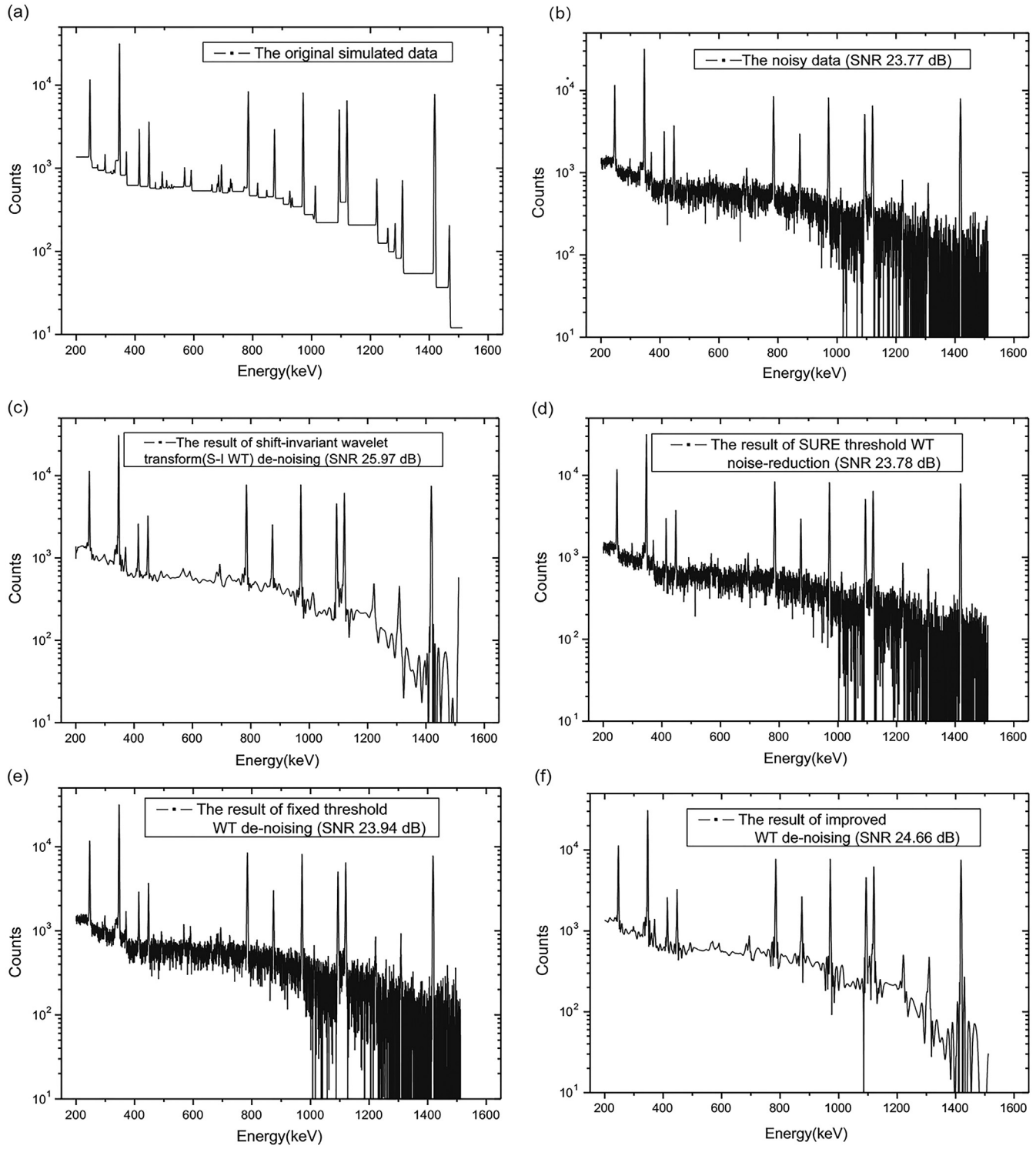

Fig. 1. The features of performance on simulated data. (a) The original simulate data , (b) The noisy data (SNR23.77dB), (C) The result of shift-invariant wavelet transform (S-I WT) de-noising (SNR25.97dB), (d) The result of SURE threshold WT noise-reduction (SNR23.78dB), (e) The result of fixed threshold WT de-noising (SNR23.94dB), and (f) The result of improved WT de-noising (SNR24.66dB) [59].

The Wavelet Fourier and other methods

In 2004, for the low-level gamma spectrum, Xiao Gang et al. proposed a nonlinear wavelet method, using the mother wave function to expand the wavelet decomposition square integrable function, respectively using wavelet smoothing method and the traditional five-point smoothing method to calculate and analysis the spectrum peak height at 1332 KeV of ^{60}Co and FWHM [49]. The peak height and FWHM obtained by nonlinear wavelet method were 992.42 and 10.06 respectively while obtained by five-point smoothing method were 997.00 and 9.92. The results showed that comparing with traditional denoising method, the nonlinear wavelet method can eliminate the statistical fluctuation, the peak loss and the peak distortion was smaller, and identify weak peaks and distinguishing overlapping peaks on the high background gamma spectrum.

In 2006, Cairo proposed a new fundamental principle based on

Table 1
The results of the comparison of WT, improved WT and S-I WT method [59].

Algorithm	Peak position (keV)	Net peak area (cps)	RMSE	AC of Fe	Relative error of AC
Original data	1173.24	2.6338	0	0.44810	0.04600
	1332.50	3.0449		0.43870	0.10630
WT	1173.24	0.8290	2.785e−2	6.23750	13.5610
	1332.50	0.7190		6.82150	16.2040
Improved WT	1173.24	2.6504	1.012e−3	0.42632	0.00481
	1332.50	3.0240		0.38022	0.04109
S-I WT	1173.24	2.6494	8.750e−4	0.42821	0.00040
	1332.50	3.0449		0.39558	0.00234

Original data: the spectrum of the transmission source ^{60}Co of the empty drum.
WT: wavelet transform.
Improved WT: improved wavelet transform.
S-I WT: shift-invariant wavelet transform.
Peak position: the highest energy of the spectrum.
RMSE: root mean square error.
AC: attenuation coefficient.
Relative error: the relative errors before and after the application of a denoising algorithm.

Fourier Transform with the purpose of solving problems of smoothing and denoising in the gamma spectrum [50]. This method was used to distinguish the two processes of smoothing and denoising. The results showed that the method almost can remove noise completely without destroying the peak value, and verified that the improved Fourier transform method can remove noise and retain peak shape better.

Since 2000, the studies of principal component analysis (PCA) applied in data treatment started to grow [51–55]. Hee-Jung Im et al. applied PCA to real-time gamma spectroscopy noise reduction in 2007, especially for gamma spectroscopy noise reduction obtained in a short time [56]. The research showed the signal noise ratio was gradually increased according to the increased measurement time, and it was enhanced by about a factor 6 times from the noisy prompt gamma spectra after the noise reduction. The majority of the noise was discarded while retaining relevant information, improving the signal-to-noise ratio (SNR).

In 2010, T. Burr et al. proposed a new two-stage smoothing program based on multiplication deviation correction (MBC) [57]. During the process, MBC was used for initialization in peak and valley values. The advantage of this approach was that it provided an adaptive smoothing by “reducing smoothness” at the peak. RMSE of wavelet algorithm without MBC is 1.34 while it is 0.91 after application. From quantitative analysis, MBC can reduce deviation, and variance can be ignored when reasonable initial smoothing device was applied in the process. This method can improve smoothing performance measured by the root mean squared error (RMSE).

In 2013, Jinzhao Zhang et al. proposed a novel shift invariant wavelet denoising algorithm [58]. In high resolution gamma spectrum denoising, the least square method can keep the shape of the spectrum, but cannot eliminate statistical fluctuations. The traditional wavelet transform denoising could lead to Gibbs phenomenon, in which the data becomes larger on both sides of the peak value, affecting the effect of denoising.

Taking ^{60}Co as an example, the peak relative error calculated by this method was 0, which was much smaller than the least squares filtering and the traditional wavelet transform. The minimum RMSE was $8.74953e^{-4}$, indicating that the shift invariant wavelet transform filtering had the highest similarity with the original data, and the data was reliable [58].

In 2016, Huailiang Li et al. proposed an improved threshold-offset invariant wavelet transform denoising algorithm and named S-I WT [59]. In this work, a common estimation algorithm was adopted to subtract background through the universal threshold (as an improved WT de-noising), defined as the formula [60]:

$$\lambda = \sigma\sqrt{2\log_2 N}$$

where λ states a threshold value, N states channel number of the spectrum, σ states standard deviation of noise. In addition to the standard de-noising technique operating with the threshold, they used a protocol applied to the wavelet coefficients. Based on the preprocessing of the gamma-ray spectrum measured by the segmented gamma scanning (SGS) system, the improved wavelet transforms and shift invariant wavelet transform were used. The smallest attenuation coefficient relative errors with the peak area are obtained.

The core algorithm of S-I WT took advantage of the time-domain translation and the decomposition scale by using these formulas:

$$S_h(x_t) = x(\ell + h) mod N$$

$$S - h(x\ell) = x(\ell - h) mod N$$

where x_t ($0 \le t \le N$) states signal, N states channel number of the spectrum, S_h states a shift operator with a cyclic shift quantity of h. The artificial oscillation amplitude was minimized by selecting the optimal translation parameter h.

They evaluated the performance of their proposed algorithm on simulated data. The features were shown in Fig. 1(a)–(f).

The S-I WT was characterized by significantly improved SNR. The denoising effects of improved WT and S-I WT were better than Stein unbiased risk estimator (SURE) and fixed-threshold WT methods. Consequently, SURE and fixed-threshold WT methods were not considered hereafter.

They took ^{152}Eu spectrum as an example to compare the denoising effect of this method with others, and the results were shown in Table 1. The RMSE of the result obtained by this method was $8.750e^{-4}$, which was much smaller than the RMSE obtained by the improved wavelet algorithm and the traditional wavelet algorithm. Moreover, statistical fluctuations were significantly reduced compared to conventional methods. The method can be used for high-resolution gamma spectroscopy and reduce the signal generated by pseudo-Gibbs artificial fluctuations.

In 2017, Yang Jia et al. used the noise adjusted singular value decomposition (NASVD) method to process ground gamma spectroscopy noise [61]. This method was a multivariate statistical analytical method, which extracts the main components of the spectral lines that were mutually orthogonal in the data set. According to the shape characteristics of each principal component, spectrum data was reconstructed only by low order principal components.

In the experimental part, the measured gamma spectrum data set constituted the matrix $A = (a_{ij})_{m\times n}$, and the variance normalization was performed.

The process is to sum the column elements in matrix A to get the $S_1^T = (s_{11}, s_{12}\cdots, s_{1n})$, to normalize and get$S_{1unit}^T = S_1^T \tilde{A}\cdot \sum_{j=1}^{n} s_{1j}$. Then to sum each row in matrix A to calculate $C_1 = (c_{11}, c_{12}, \cdots, c_{m1})^T$. A corresponding average spectral matrix can be regarded as $C_1 S_{unit}^T$, and the unit variance matrix ANA can be expressed as$[\frac{a_{ij}}{\sqrt{(C_i S_{1unit}^T)_{ij}}}]_{m\times n}$.

The standard three-window method was used to compare the noise reduction results of the NASVD method with the noise reduction results of the traditional LS method, and respectively obtained the count values of the potassium window, the uranium window, and the thorium window.

The results showed that the net peak area value of each window after NASVD noise reduction was closer to the real data, which can significantly reduce the statistical fluctuations in the original data, and it was more suitable for the noise reduction processing of the ground gamma spectrum single measurement data.

At present, LS fitting smoothing and traditional wavelet transform processing energy spectrum data are common denoising processing methods. The LS method can be used for curve fitting, but there are still

some shortcomings. In the process of denoising, it is easy to deform the spectrum, lose weak peaks, reduce the accuracy of the spectrum and generate a large error. The traditional wavelet transform causes the pseudo-Gibbs phenomenon at the discontinuous point of the signal after denoising. Based on these two methods, improvements proposed by spectroscopists and researchers have subtly avoided the previous adverse effects. The new method is constantly being proposed, and the authors believe that it worth effort to deeply study on retaining the peak shape to the greatest extent without losing the weak peak, making the RMSE as small as possible.

Background subtraction

The background is mainly due to Compton scattering effect, small angle scattering of gamma rays in the sensitive volume of detector and other interference factors in the energy range of gamma spectrum [62]. Due to the photoelectric effect, Compton scattering and electron pair effect, gamma rays scatter with the periphery and the detector, lower energy scattering photons and recoil electrons are generated. The random scattering angle of the Compton Effect is reflected in a continuous flat (Compton platform) on the spectrum. In the process of small angle scattering by a gamma ray in the sensitive region of the detector, quantum photon energy loss is very small, resulting in high/low energy trailing phenomenon in the measured characteristic peak [63,64]. Every γ-ray source class makes a different contribution to the γ-ray background [65]. In addition, external factors of radioactive sources, such as radionuclides in the environment, noise caused by electronic instruments, cosmic rays, electromagnetic interference, etc. [66–72], will generate environmental background, while internal factors of radioactive sources will lead to the appearance of radioactive background [73]. Since radionuclides are always loaded by the carrier, in addition to the radionuclides to be measured, a large number of other radionuclides exist in the source, and count interference will occur.

The scattering background increases the complexity of the gamma spectrum, making it difficult for some weak peaks to be discovered and affects the accuracy of spectrum analysis. In the process of analyzing the spectrum, in order to eliminate useless spectral data and improve the measurement accuracy of the spectrometer, the most fundamental problem is to separate background from valid data and subtract [74–77]. In order to improve the accuracy of radionuclide concentration analysis, it is necessary to effectively identify and subtract the count independent of the characteristic peak area [78]. In a broad sense, the count of any cause other than the radionuclide to be measured can be considered as background. Aiming at the background subtraction, a series of methods including parabola background subtraction [79], peak clipping [80], filtering method [81], iterative method [19], SNIP and its related derivative methods [17,82–87] and Fourier transform [88,89] are proposed.

SNIP methods

In 1988, C.G.R. proposed the principle that based on the algorithm of Sensitive nonlinear iterative peak (SNIP), the background of gamma spectrum can be subtracted. The algorithm of SNIP is believed to be able to remove the background. However, in terms of details, the SNIP algorithm is affected by the peak area width parameter N, and different backgrounds are subtracted when different N parameters are selected [17]. Subsequently, Morhac et al. improved this method in 1997. They used the LLS (twice log operators plus square-root operator) operator firstly to improve the SNIP algorithm to the weak peak [88]. Before applying SNIP algorithm, the LLS operator is used to transform each energy spectrum count with the formula:

$$V(i) = \log[\log(\sqrt{y(i)+1}+1)+1]$$

where i represents the channel, y(i) are the energy counts in the channel i, V(i) is the saving vector after y(i) is transformed by LLS operator, then $V_1(i)$, $V_2(i)$ are calculated up to $V_m(i)$ step by step, where, m is a given free parameter, and it is generally the FWHM. The new value in the channel i in the p-th iteration is obtained by the formula:

$$V_p(i)=\min\{\frac{1}{2}[V_{p-1}(i-p)+V_{p-1}(i+p)],\ V_{p-1}(i)$$

where p grows iteratively from 1 to a given m value with step size 1. When $V_m(i)$ is calculated, the net value of the spectrum can be obtained by performing the inverse calculation of LLS operator. Also the algorithm was deduced that could deal with not only one-dimensional spectrum but also multi-dimensional spectrum, the algorithm must be able to recognize not only continuous background but also to include all the combinations of coincidences of the background in some dimensions and the peaks in the other ones [82].

In 2009, Morhac et al. proposed a new SNIP algorithm with a clipping window adaptive to peak regions widths, to deal with the situation that if there was an inaccurate value m [83]. In this research, he assumed that k peak regions have been identified, and then constructed vector with length n, and the vector r can be defined by formula:

$$\mathbf{r} = [0, 0, ...0, W_1, ...W_1, 0, ...,0, W_2, W_2, ...,W_2, 0, ...,0, ...0, ...0, W_k, W_k, ...W_k, 0, 0, ...,0]^T$$

where "0" is located in peak free area, W_j represents the width of the j-th peak area and is located in the j-th peak area, and $m = \mathrm{Max}\{W_j\}$, $j \in (1, k)$, the modified SNIP method can be expressed as:

$$y_p(i) = \begin{cases} min\left\{y_{p-1}(i), \frac{1}{2}[(i+p)+y_{p-1}(i-p)]\right\} & ifp \le r(i) \\ y_p(i) & otherwise \end{cases}$$

where the p grows iteratively from 1 to the variable m, the i represents the channel, the r(i) is the biggest W_i in the vector r, and $y_p(i)$ is the saving vector after the energy counts in the channel i is transformed by LLS operator.

The ability of estimating background was compared by using the proposed methods with increasing clipping window (the window was changing starting from the value 1 up to the given value m) and decreasing clipping window (the window was changing starting from the value m up to the given value 1), the results were shown in Fig. 2(a) and (b). It was apparent that the estimate of decreasing clipping window implemented more reasonable.

Another further comparison between using the traditional SNIP algorithm and using the improved SNIP algorithm with decreasing clipping window was given. The results were shown in Fig. 3(a) and (b).

It could be seen that the improved algorithm subtracted the background more thoroughly and accurately, and it could avoid some false peaks, the data of the background wouldn't be affected by a rough value m.

Moreover, Morhac et al. made a series of improvements to the SNIP algorithm, they replaced the function in the original SNIP algorithm with a higher-order filter function for better baseline estimation effect. Therefore, the contradiction of fixed window width was alleviated to some extent when applied to different energy zones. Which allowed estimation of specific shapes of background and ridges as well [84].

In 2013, B. Long, used symmetric zero area for peak method to calculate the different period of characteristic peaks corresponding to the peak width, then adopted SNIP method for scattering background subtraction [85]. It this research, the effect of peak width at scattering background was solved, and the adaptive subtraction of scattering background was realized. The spectrum processing was compared by this method and Genie 2000, and the relative difference between the net area of the characteristic energy peak was found to be less than 2%. When using Genie 2000 to subtract the background, the net peak area can be written as the following formula.

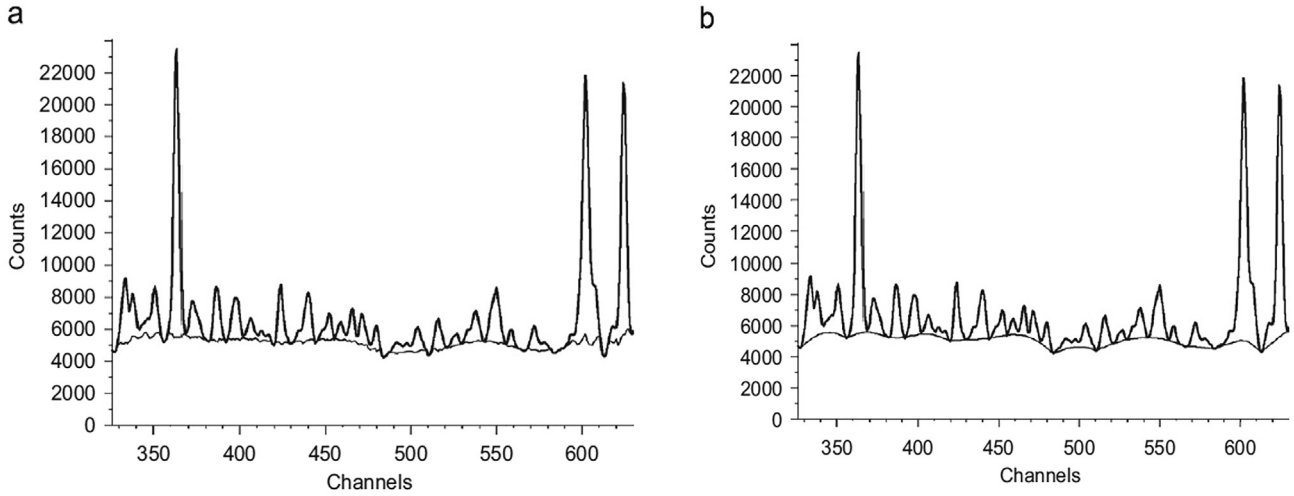

Fig. 2. An example of γ-ray spectrum with estimated background using alterable clipping window. (a) Using increasing clipping window, (b) Using decreasing clipping window [83].

$$S = R\left[G - \left(\frac{N}{2n}\right)(B_1 + B_2)\right] - \frac{T_s}{T_b} I_b$$

where G is the gross counts in the peak region of interest (ROI), N is the number of channels in the background peak ROI, n is the number of continuum channels on each side, B_1 is the sum of counts in the low energy continuum region, and B_2 is the sum of counts in the high energy continuum region T_s is the live time of the sample spectrum, T_b is the live time of the background spectrum, I_b is the net peak area of the peak in the background spectrum.

In 2016, Meng-Hua Zhu et al. considered the inverse cumulative accumulation process (ICAP) and put forward a new method to avoid calculating the FWHM of the whole spectrum. Through the filter, the peak was smoothed constantly until the background was a straight line. This method was able to deal with the case that the peak was too small to estimate the FWHM. In addition, by combining the proposed method and the SNIP method, the average FWHM can be determined easily, and eventually the date of the background can be obtained conveniently [62].

In 2018, Rui shi et al. invented a method to calculate and subtract the gamma spectrum background by successive approximation SNIP, and improved this method by using the adaptive peak area width of filter window [86]. In this study, successive approximation was used to improve the accuracy of the background subtraction, until the relative error of the area of the background obtained by two operations was no more than 0.5%. No calculation parameters need to be selected artificially in this algorithm, and the background directly subtracted after the first calculation was regarded as a new energy spectrum for calculation. The iteration termination condition was not a fixed number of steps, but the algorithm stopped after a certain accuracy was satisfied.

Other methods

In 1981, Steenstrup proposed a background estimation method, which used orthogonal polynomial to fit the spectrum and repeated adjustment of the coefficient of the least square fitting to achieve the trace address with background only included in the fitting [90]. This method was applied to the pulse spectrum, which was relatively easy to complete with little or no parameters.

In 1983, D.D. Burgess used the zero-area digital filter to estimate the background of the energy spectrum in a specified range of upper and lower limits. However, in the case that the specific resolution of the detector was not clear, this method cannot accurately estimate the location of the background and cannot resolve the situation when the peak width was too narrow [91].

In 1987, Claytonetal put forward a kind of “off peak” based on stripping the rapidly changing characteristic information in the energy

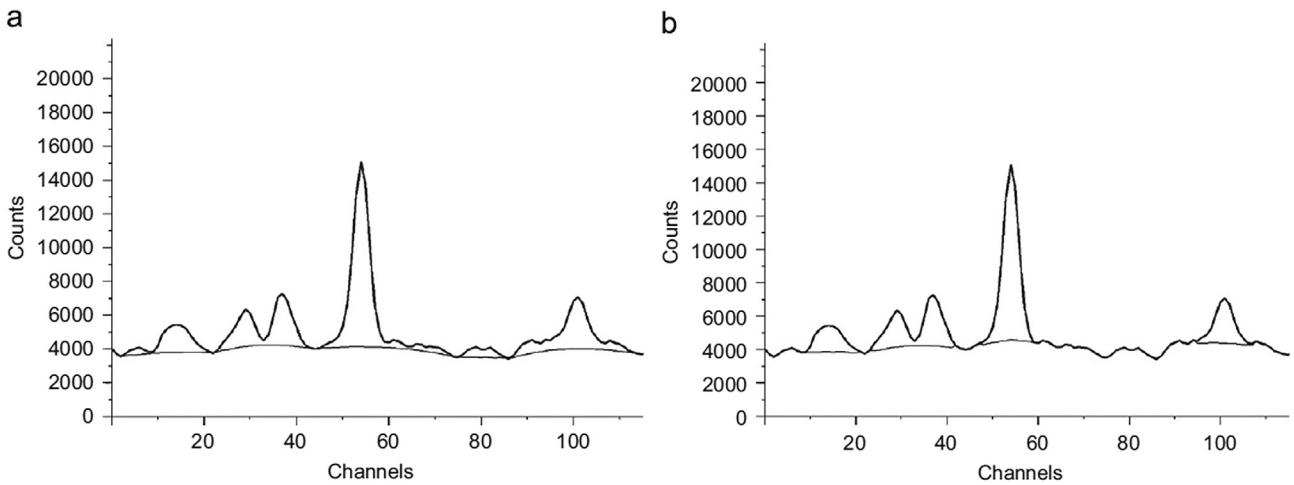

Fig. 3. Experimental γ-ray spectrum with estimated background using traditional SNIP algorithm (a) and using the improved SNIP algorithm (b). (a) Using fixed width of clipping window given as user defined parameter, (b) Using the decreasing clipping window automatically adjustable to the widths of the peak regoons [83].

spectrum [92]. By comparing the channel i with its two neighboring channels' average, replacing the larger value with smaller value, and ran the suitable times repeatedly on the whole spectrum to get the background, it avoided the error due to the use of different accurate mathematical model. Before stripping the spectral line, the number of iterations can be reduced by taking the logarithm or the number of squares of the data. The time of cycles of the spectral line depends on the width of the peak.

In 2008, Zhu M.H. et al. used an iterative method to estimate the width of peak regions for the background elimination of γ-ray spectrum [93]. The methods were divided into four parts: (i) searching for peaks to obtain the initial regions in the whole spectrum. (ii) merging adjacent regions where cross values occurred. (iii) using a heuristic approach to obtain the real width of each region with two directions. (iv) checking whether two adjacent corrected regions had the same background. The background was estimated approximately linearly under the peaks in each region, which made it was able to distinguish each peak clearly.

Based on C.V. Hampton's study [88], Zhang Qingxian et al. used the Fourier transform to subtract the background in 2012. The Fourier transform could get the background without calculating the effective peak width, and the estimated error of the background was within 11% compared when the estimated error by using liner methods was about 25.9%, which meant it had a good background elimination capacity [89]. However, the expression of the Fourier transform in the lower energy segment was not sufficient, due to this the use of the Fourier transform method had some limitations.

Besides various iteration algorithms, the SNIP algorithm and its variants are considered as a widely acceptable gamma spectrum background subtraction method. Because of the algorithm characteristic, SNIP can subtract the background completely if the given parameter m is accurate. However, an inaccurate parameter can lead to different subtraction efficiency in different energy segments. Much work has been done to improve this algorithm by reducing the effect of parameter m, and the SNIP algorithm is approaching complete without the influence of precondition to deal with more sophisticated situation. Therefore, we believe it is worth to study a potential method which can subtract the background without giving an artificial parameter.

Overlapping peak separation

Due to the multiple factors (such as spectral resolution limitations of the instrument, existence of the detector's dead layer, particle piled caused by the incomplete absorption of electric charge, and complex components of the target), overlapping peak separation is a common and inevitable conundrum in gamma spectrum unfolding technique. In addition, the reaction between gamma ray and matter produces the Compton effect, resulting in indefinite scattering angle. In a complex sample, continuous Compton platform created by different elements increases the difficulty of overlapping peak separation. Similarly, the sample itself leads to the phenomenon that characteristic peaks of adjoining elements stay close in the spectrum, which may result in errors in the spectral extraction peak parameter and sample component analysis. The overlapping peaks separation method is a key point to the gamma ray spectrum unfolding technique, the evaluation criterion of the method is the resolution accuracy. However, the accuracy of the identification and separation of overlapping peaks makes different analytical results due to different methods [94]. Therefore, researchers put more attention in using different mathematical methods to process the spectral data to improve the separation accuracy of the original overlapping peak.

Many different improvements have been proposed for the analysis of overlapping peaks, such as wavelet transform, Fourier auto-reverse convolution [95], curve fitting [21,96,97], improved vertical line method and tangent method, trigonometric method [98], deconvolution [99,100,101], etc., Though these analytical methods for overlapping peaks have their own limitations, method like peak fitting can still be used in overlapping separation because of its high accuracy in peak parameter extraction. Its related functions have become an essential analysis module for many software that has been widely used in practical applications. Nevertheless, this kind of processing requires the operator to specify the peak position and other parameters, which cannot meet the requirements for in-situ detection and on-site automated analysis.

Geometric methods

The current prevailing overlapping peak separation method can be divided into two categories: geometric method and algebraic method [102]. The geometric method is mainly based on calculating the peak height of a single peak in overlapping peaks. In general, the geometric method can be divided into vertical line method, tangent method and trigonometric method. On count of its visual and fast calculating speed, geometric method is often used in real time online data processing [98]. However, the accuracy of the peak separation of the geometric method varies with the overlapping extent of the peaks. When the peak overlap is severe, the calculation accuracy of each peak area cannot meet the demand.

Ekaterina Larionova et al. evaluated the peak height by applying tangent the method in 2013. In this study, the undefined peak can be observed, but the conventional peak height measurement was impossible. It was recommended to estimate the maximum peak at the inflection point of the curved tangent drawn for the frame height at the peak branch and thus propose a systematic error compensation method. The maximum overlapping peak was measured by using the system error compensation technique combined with the tangent method. Its purpose was to exclude in some cases the necessity of calculating the resolution of a mathematical or chemical overlapping peak and the range extension of the calculated concentration, the value of the resolution and the ratio of the peak height [98]. In addition, Ye Guoyang et al. proposed the intersection vertical method and the proportional distribution method for overlapping peaks in 2016, which greatly improved the peak separation accuracy. In this research, the baseline was corrected by using asymmetric least squares method and group peak baseline method [103]. The intersection perpendicular method and the proportional distribution method were proposed for overlapping peaks, which effectively improved the peak accuracy. The error of the vertical method was less than 28.688%, and the error of intersection vertical method and proportional distribution method was within 5%, which can speed up the analysis to ensure real-time performance.

The geometric method can improve the calculation speed to make the analysis clearer visually and to guarantee the real-time results. The accuracy of peak segmentation and area calculation is improved. But the resolution accuracy varies with the degree of overlap. When the chromatographic peaks overlap seriously, the calculation accuracy of each peak area has a large error, and it is more complex and difficult to operate in practical problems.

Algebraic methods

The most commonly used algebraic methods are function fitting method and wavelet transform method. The principle of function fitting method is to determine the function model of the peak pattern, and to use the least squares method (LSM) to fit the overlapping peak data, meanwhile, to adopt some optimization methods to optimize all the parameters. These parameters can be determined through continuous iteration, and the fitting curve can be continuously approached to the actual curve. Eventually, a set of optimal estimates is obtained, based on those parameters the area of each sub-peak can be calculated. In this review, we mainly focus on the application of the geometric method.

Function-fitting method

Alfonso Fernández-González et al. found that the first derivative method usually cannot detect overlapping peaks in 2009, especially when they appeared on the shoulder of the main peak, so he proposed an accurate estimation method of peak position based on Gaussian curve linearization and named it Natural Logarithm Derivative Method (NLDM), which can detect overlapping peaks to some extent. The Lorentz influence, the experimental error in the numerical calculation, and the minimum separation between peaks that influence the peak shape was studied to achieve a reasonable solution [104]. H.C. Goicoechea et al. proposed a second-order algorithm for the distinguishing and explaining of overlapping peaks in 2010. In addition, these algorithms were useful when the data had no third-order linearity, and time shift correction was not needed. Therefore, this thought was a more effective method for dealing with matrix effects and had been successfully applied in the analysis of complex samples combining with second-order algorithms [94].

Wang Guowei et al. studied the linear sweep volumetric peak (LSVP) overlap problem of small signal overlap to large signal overlap in 2015 based on the high signal overlap linear sweep volumetric solution method according to the state transfer algorithm, and proposed a state transfer algorithm-based parameter optimization method, by which the overlapping LSVP can be decomposed into independent sub-peaks [105]. The results showed that the fitting degree of describing the overlapping LSVP was greater than 97%. The proposed method was reasonable and effective for the solution of overlapping LSVP in the case of high signal to noise ratio greater than 50.

In 2016, Joseph Dubrovkin proposed a resolution method for overlapping linear sweep polarographic peaks based on the Gaussian distribution. In this study, nonlinear weighted least squares method was used to fit the curve and its derivative curve. Meanwhile, without introducing errors, it was found that these estimated peak intensities and area increments were inversely proportional to the square root of the peak width. The estimated maximum peak and width increments were approximately proportional to the square root of the peak width and inversely proportional to the peak intensity, which enabled researchers to significantly reduce the size of the data set used to model the analysis signal [106,107]. The overlapping peaks were decomposed into independent sub-peaks according to the fitting reconstruction parameters. The experimental results showed that the relative error of the half-wave potential determined by multi-resolution wavelet decomposition was less than 1%, and the accuracy of nonlinear weighted least squares (NWLS) fitting was higher than 96%. By constructing an asymmetric distribution, the resolution of overlapping peaks was successfully extended to the asymmetric sub-peak field, which provided a reference for other overlapping peaks composed of asymmetric sub-peaks [108,109].

Continuous wavelet transform and its variants

Continuous wavelet transformation (CWT), as an important time-frequency analysis tool, has been widely used in signal processing to divide continuous-time signals into scale wavelets and translation wavelets so as to obtain a two-dimensional coefficient matrix. Additional information can be obtained through conversion to the time-frequency space, which makes peak detection simpler. Mathematically, this process of CWT is represented as the formula.

$$C(a, b) = \int_{-\infty}^{+\infty} s(t)\psi_{a,b}(t)dt,\ \psi_{a,b}(t) = \frac{1}{\sqrt{a}}\psi(\frac{t-b}{a}),\ a \in R^{+},\ b \in R$$

where s(t) means the signal, a is the scale, b is the translation, ψa, b(t) is the mother wavelet after the scale transformation C(a,b) is a two-dimensional coefficient matrix [110,111,112].

It is assumed that Fourier Support is divided into continuous segments. Each segment (ω0 = 0 and ωN = π) is defined as the segmented Fourier spectrum. The nth segment is used to indicate the use ofΛn = [ωn − 1, ωn]. A transition phase Tn of width τ_2 n is centered around each ωn. The empirical wavelet is defined as each bandΛn with bandpass filter. In order to get the empirical wavelet, Littlewood-Paley and Meyer wavelet are adopted. ∀n > 0, the empirical scale function and the empirical wavelet are acquired from equations [113–117].

$$\hat{\phi}(\omega) = \begin{cases} 1 & \omega| \leqslant (1-\gamma)\omega_n \\ \cos[\frac{\pi}{2}\beta(\frac{1}{2\gamma\omega_n}(|\omega| - (1-\omega)\omega_n))] & (1-\gamma)\omega_n \leqslant |\omega| \leqslant (1+\gamma)\omega_n \\ 0 & otherwise \end{cases}$$

where we choose τn to be proportional to ω_n: τn = γω_n, and 0 < γ < 1 , ω is the frequency, $\hat{\phi}(\omega)$ is the length at which $\hat{\phi}(\omega)$ converges from a finite value to 0 as time or frequency approaches infinity.

And

$$\hat{\psi} = \begin{cases} 1 & (1+\gamma)\omega_n \leqslant |\omega| \leqslant (1-\gamma)\omega_{n+1} \\ \cos\left[\frac{\pi}{2}\beta\left(\frac{1}{2\gamma\omega_n}((|\omega| - (1 - \gamma)\omega_{n+1})\right)\right] & (1-\gamma)\omega_{n+1} \leqslant |\omega| \leqslant (1+\gamma)\omega_{n+1} \\ \sin[\frac{\pi}{2}\beta(\frac{1}{2\gamma\omega_n}(|\omega| - (1-\gamma)\omega_n))] & (1-\gamma)\omega_n \leqslant |\omega| \leqslant (1+\gamma)\omega_n \\ 0 & otherwise \end{cases}$$

where we choose τn to be proportional to ω_n: τn = γω_n, and 0 < γ < 1, ω is the frequency, $\hat{\psi}$ is the length at which $\hat{\psi}$converges from a finite value to 0 as time or frequency approaches infinity.

β(x) is defined as follows:

$$\begin{cases} \beta(x) = 0 x = 0 \\ \beta(x) + \beta(1-x) = 1,\ \forall\ x \in (0, 1) \\ (x) = 1 x = 1 \end{cases}$$

Li Yuanlu used Haar wavelet as a tool to design a fractional-order differentiation filter for establishing Fractional Derivative Spectrum (FDS), in order to solve overlapping peak separation [118]. FDS was allowed to specify the most appropriate fit model and obtained its peak parameters in a unique way. For unknown overlapping bands, the method was to separate overlapping peaks from left to right. After separating a peak from the original overlapping peak, one peak can be used to subtract one peak to separate the other one. Repeating the steps until all peaks are separated. This method cannot only maintain the advantages of the derivative spectroscopy method, but also gain the characteristic parameters of the single band (see Table 2).

The Mexican hat wavelet (Fig. 4(a)) is usually chosen as the mother wavelet because of its Gaussian MS peak characteristics, such as approximate symmetry and a major positive peak. Fig. 4(b) is a CWT coefficient matrix of the mass spectrometry (MS) peak of the signal simulated by the Gaussian function. Ying Zheng et al. found the higher the coefficient, the better the match between the signal and the mother wavelet. At the same time, more true peaks can be detected while maintaining a low false discovery rate of CWT [119].

Liu Minghui proposed an overlapping peak separation method based on Lorentz4 wavelet transform method. The method identified peaks by plotting ridge lines in the Lorentz4 wavelet space of the degenerate Raman spectra. The performance of the proposed method was evaluated by Raman spectra, of which the results indicated that the CWT peak detection method based on the new Lorentz4 wavelet was better than the two commonly used wavelets in detecting the overlapping peaks (see Fig. 5). This method can maintain the low false discovery rate, while detect more true peaks [22].

Jiao Long et al. found that the problem of overlapping peaks can be easily solved by converting experimental signals into wavelet coefficients [120]. The application of this method to the measure of overlapping peaks had a satisfactory quantitative result. Compared with the quantitative results of numerical differentiation method, CWT has been proved to be able to suppress signal noise and improve the resolution of overlapped peaks.

Table 2
The original peak parameters, peak parameters obtained by estimator II and their relative error [118].

Separating degree		Original parameters			Processed parameters			Relative error(%)		
		μ	A	O	μ	A	O	μ	A	O
(a) 0.25	Left peak	−0.5	5.0	1.5	−0.4812	5.1140	1.4943	3.7582	2.2804	0.3826
	Right peak	0.5	1.0	0.5	0.5143	0.9530	0.4846	2.8505	4.7038	3.0715
(b) 0.5	Left peak	−0.5	5.0	1.5	−0.5060	5.0161	1.4896	1.2037	0.3226	0.6921
	Right peak	1.5	1.0	0.5	1.5111	1.0095	0.4917	0.7390	0.9457	1.6678
(c) 0.75	Left peak	−1.5	5.0	1.5	−1.5081	5.0125	1.4898	0.5389	0.2492	0.6810
	Right peak	1.5	2	0.5	1.5111	2.0147	0.4914	0.7417	0.7364	1.7280
(d) 1.0	Left peak	−1.5	5.0	1.5	−1.5104	4.9929	1.4891	0.6956	0.1428	0.7283
	Right peak	2.5	2	0.5	2.5112	2.0140	0.4913	0.4461	0.7002	1.7360
(e) 1.25	Left peak	−2.5	5.0	1.5	−2.5112	4.9888	1.4891	0.4481	0.2237	0.7280
	Right peak	2.5	2	0.5	2.5112	2.0123	0.4912	0.4490	0.6140	1.7542
(f) 1.5	Left peak	−2.5	5	1.2	−2.5104	5.0186	1.1909	0.4174	0.3720	0.7607
	Right peak	3.5	4	0.8	3.5115	4.0016	0.7904	0.3276	0.0390	1.1972

Original parameters: The data measured by the experiment.
Processed parameters: The data measured by MATLAB.
Relative error: Defined as $(X_2 - X_1)/X_2 * 100\%$, where X_2 is original parameters, X_1 is processed parameters.
μ: the peak of the adjacent peak of the Lorentz peak.
A: the amplitude of the Lorentz peak.
O: the half width of the Lorentz peak.

Overlap phenomenon is very common in gamma-ray spectrum analysis, which makes further qualitative and quantitative analysis difficult. For such problems, the development of instruments to improve signal resolution is often limited by practical problems or working conditions. Therefore, the accuracy is usually improved by improving experimental methods and mathematical operations. Among them, the least squares method is often used as the evaluation standard to judge the fitting effect, but when the components overlap seriously, the small error in the experimental data will also lead to the large fluctuation of the results. Derivative method is a mature method to identify overlapped peaks. However, as the number of derivatives increases, the noise will enhance. In higher derivatives, the signal may be completely covered by noise. The wavelet analysis and its improvement methods are commonly used to solve the problem of overlapping peaks, obtaining additional information by time-frequency space transform to detect spectrum data processing, an advantage of using the mathematical method of overlapping peaks decomposition is hardware requirements is not high, as long as under certain conditions, using the mathematical method to calculate, can get enough data, the result of the higher precision is achieved. However, the selection of wavelet basis is not a standard system and it is time-consuming and relatively one-sided. And the low degree of separation effect of overlapping peak is not obvious, which can obtain the results of overlapping peak analysis with higher accuracy and basically meet the detection and analysis of general requirements. Therefore, the author believes that wavelet analysis and its improved method are more practical overlapped spectral analysis peaks of the problem.

Conclusion

We briefly discussed gamma spectrum unfolding algorithms and their applications and the focus is on the denoising, background subtraction and overlapping peak separation. We mainly introduce the basic mathematical models and their correlation formulas, analyze the improved algorithms and methods in more details, result the following conclusions.

(i) Traditional gamma spectral data smoothing is carried out in the

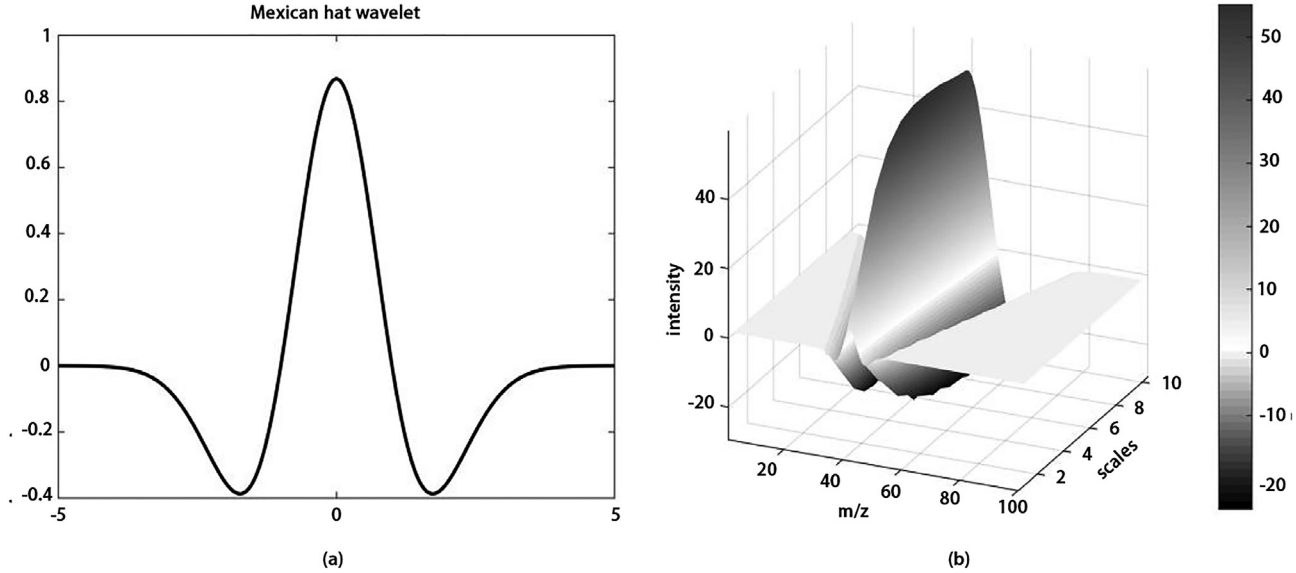

Fig. 4. The Mexican hat wavelet (a) is usually selected as the mother wavelet because of the features of Gaussian MS peaks, such as approximate symmetry and one major positive peak. (b) is the CWT coefficient matrix of a signal MS peak simulated by a Gaussian function [119].

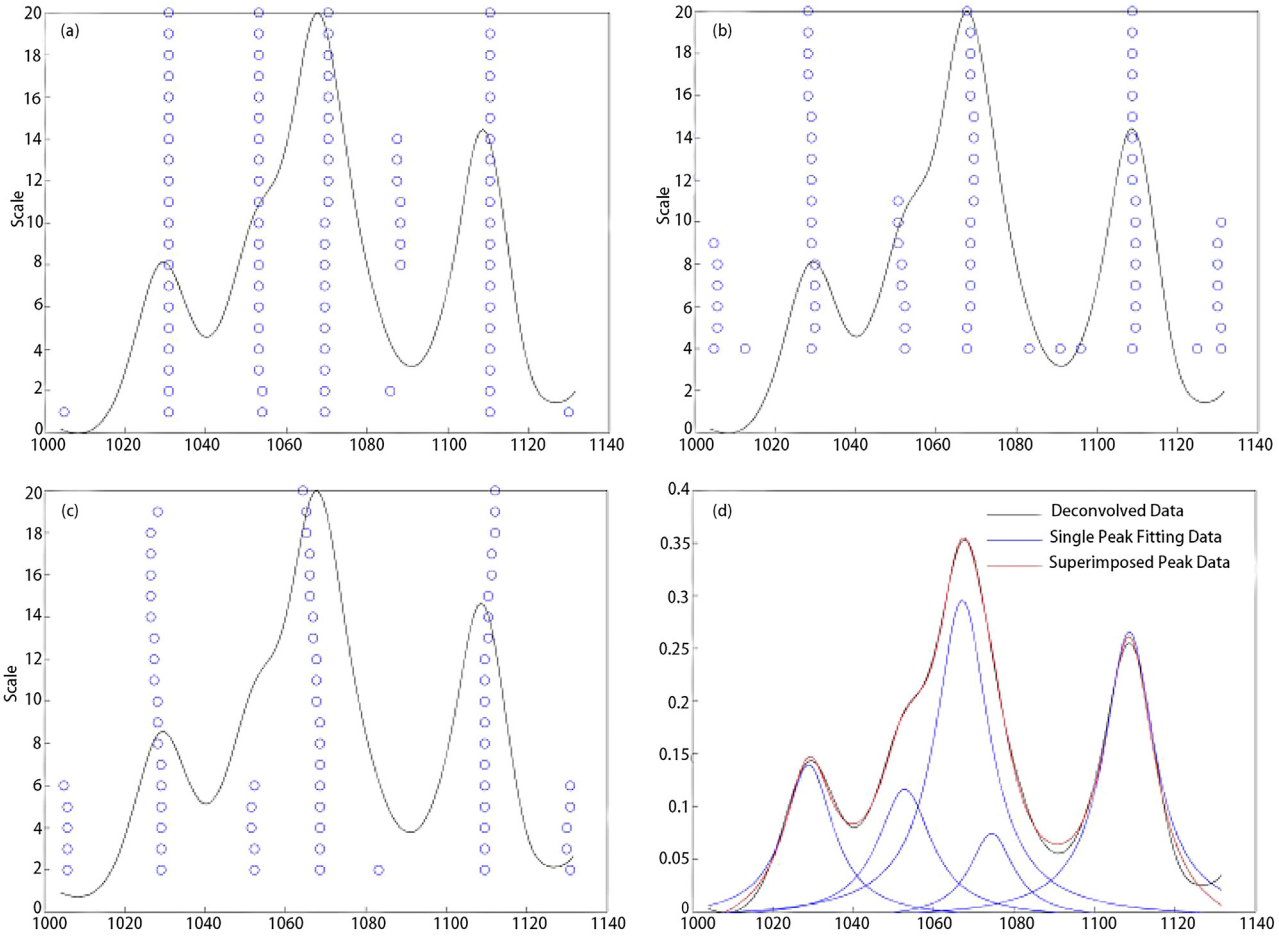

Fig. 5. Comparison of three wavelets in the CTW-based peak detection method for overlapping peaks. (a) Lorentz4 wavalet, (b) Guas4 wavelet, (c) Mexican hat wavelet, (d) Fitting peaks [22].

channel domain or frequency domain and causes large spectral distortion because of their limited adaptability. Throughout the smoothing process, the constant weighting coefficient may lead to the loss of weak peaks or the appearance of false peaks. Because the same smoothing process is applied to each channel and the degree of influence on the spectral line changes with the intensity of the spectral line, it is not conducive to subsequent qualitative and quantitative analysis. Improved methods such as RLS-SVM, S-I WT, NASVD, etc. are proposed to improve the adaptability and retain the useful information to the greatest extent.

(ii) Background subtraction is an important link in the analysis of γ-ray spectrum. The common dispose of background usually has difficulties to distinguish the true and false peaks, leaves much invalid data and the effective part of the spectrum. Methods based on SNIP algorithm have good precision and background subtraction efficiency. However, an important parameter in the algorithm should be given artificially, this leads to the lack of adaptability and the ability to handle complex spectrum. Improved methods are generally proposed subtracting the background by integrating other mathematical means (LLS, clipping window, filter function, etc.).

(iii) Geometric and algebraic methods (WT, Fourier transform, deconvolution, etc.) are proposed to solve overlapping peak separation. Specially wavelet analysis is an effective combination of Fourier transform, harmonic analysis and numerical analysis. It is an important time-frequency analysis tool, applied to signal processing, through the conversion of time-frequency space, additional information is obtained, making peak detection simpler. Wavelet analysis and its improved method cannot only obtain the characteristic parameters of a single band, but also detect more true peaks.

In general, for the mathematical method of qualitative and quantitative analysis of the gamma spectrum, a single algorithm cannot meet the complex spectrum unfolding requirement. Combining the advantages of different algorithms is the trend of current research to establish reasonable mathematical models objects to solve practical problems. Due to the continuously growing of gamma spectrum unfolding algorithm studies, we expect more various potential work can be developed in this field.

Acknowledgement

This work was funded by the Opening Fund of Provincial Key Lab of Applied Nuclear Techniques in Geosciences, the National Key R&D Project (No. 2017YFC0602100) and the National Natural Science Foundation of China (No. 4177040587). Also thanks to Professor Qingxian Zhang for his guidance and opinions.

References

[1] Gilmore Gordon R. Practical gamma-ray spectrometry. 2nd ed. John Wiley & Sons Ltd.; 2018.

[2] Rouzea GS, Morgana CLS, McBratneyb AB. Understanding the utility of aerial gamma radiometrics for mapping soil properties through proximal gamma surveys. Geoderma 2017;289:185–95.

[3] Cresswell Alan J, Sanderson David CW. Katsuhiko Yamaguchi. assessment of the calibration of gamma spectrometry systems in forest environments. J Environ Radioact 2018;181:70–7.

[4] Maacha L, Jaffal M, Jarni A, Kchikach A, Mouguina EM. A contribution of airborne magnetic, gamma ray spectrometric data in understanding the structure of the Central Jebilet Hercynian massif and implications for mining. J Afr Earth Sc 2017;134:389–403.
[5] Söderström Mats, Eriksson Jan. Gamma-ray spectrometry and geological maps as tools for cadmium risk assessment in arable soils. Geoderma 2013;192:323–34.
[6] Khan HM, Chaudhry ZS, Ismail M, Khan K. Assessment of radionuclides, trace metals and radionuclide transfer from soil to food of Jhangar Valley (Pakistan) using gamma-ray spectrometry. Water Air Soil Pollut 2010;213(1–4):353–62.
[7] Kovář P, Šolc J. Subtraction of natural radiation contribution from gamma-ray spectra measured by HPGe detector. Appl Radiat Isot 2018;134:167–71.
[8] Alzimami K, Abuelhia E, Podolyak Z, Ioannou A, Spyrou NM. Characterization of LaBr 3: Ce and LaCl3: Ce scintillators for gamma-ray spectroscopy. J Radioan Nucl Chem 2008;278(3):755–9.
[9] Volkovitsky P, Naudus P. Absolute 60Co characterization based on gamma–gamma coincident detection by two NaI(Tl) detectors. Nucl Instrum Methods Phys Res Sect A 2009;607(3):568–72.
[10] Barã J, Tondeur F. Gamma spectrum unfolding for a NaI monitor of radioactivity in aquatic systems: experimental evaluations of the minimal detectable activity. Appl Radiat Isot 2011;69(8):1121–4.
[11] Booth RS. A comparison of folding and unfolding techniques for determining the gamma spectrum from thermal neutron capture in aluminum. Nucl Instrum Methods 1970;85(1):69–76.
[12] Zhu MH, Liu LG, Qi DX, You Z, Xu AA. Smoothing noisy spectroscopic data with many-knot spline method. Nucl Instrum Methods Phys Res A 2008;589:484–6.
[13] Tirosh S, Ville DVD, Unser M. Polyharmonic smoothing splines and the multidimensional wiener filtering of fractal-like signals. IEEE 2006;15(9):2616–30.
[14] Claeskens G, Carroll RJ. Automatic estimation of multivariate spectra via smoothing splines. Biometrika 2007;94(2):335–45.
[15] Fan CL, Pang MY. Reconstructing smooth curve from noise sampled data. Proceedings of the 2009 international workshop on information security and application. 2009. p. 218–22.
[16] Copeland BR, Chen M, Wade BD, Powers LS. A noise-driven strategy for background estimation and event detection in data streams. Signal Process 2006;86(12):3739–51.
[17] Ryan CG, Clayton E, Griffin WL, Sie SH, Cousens DR. SNIP, a statistics-sensitive background treatment for the quantitative analysis of PIXE spectra in geoscience applications. Nucl. Inst. Methods Phys. Res. B 1998;34:396–402.
[18] Lucaa Aurelian, Morelb Jean. Influence of the background approximation methods on the analysis of γ-ray spectra. Appl Radiat Isot 2004;60(2):233–7.
[19] Zhu MH, Liu LG, Cheng YS, Dong TK, You Z. Iterative estimation of the background in noisy spectroscopic data. Nucl Instrum Methods Phys Res A 2009;602(2):597–9.
[20] Kong H, Ye F, Lu X, Guo L, Tian J. Deconvolution of overlapped peaks based on the exponentially modified Gaussian model in comprehensive two-dimensional gas chromatography. J Chromatogr A 2005;1086(1):160–4.
[21] Yaogai Hu, Li Wei, Jiming Hu. Resolving overlapped spectra with curve fitting. Spectrochimica Acta Part A 2005;62(1–3):16–21.
[22] Liu Minghui, Dong Zuoren, Xin Guofeng, Sun Yangguang, Ronghui Qu. An improved method based on a new wavelet transform for overlapped peak detection on spectrum obtained by portable Raman system. Chemometr Intell Lab Syst 2018;182:1–8.
[23] Mertens C, Lellis CD, Put PV, Tondeur F. MCNP simulation and spectrum unfolding for an NaI monitor of radioactivity in aquatic systems. Nucl Instrum Methods Phys Res Sect A 2007;580(1):118–22.
[24] Zimmerman BE. Decay data for the positron emission tomography imaging radionuclide 124I: a DDEP evaluation. Appl Radiat Isot 2018;134:433–8.
[25] Fitzgerald R, Zimmerman BE, Bergeron DE, Cessna JC, Pibida L, Moreira DS. A new NIST primary standardization of (18)F. Appl Radiat Isotopes: Including Data Instrum Methods Agric Ind Med 2013;85:77–84.
[26] Tsabaris Christos, Prospathopoulos Aristides. Automated quantitative analysis of in-situ NaI measured spectra in the marine environment using a wavelet-based smoothing technique. Appl Radiat Isotopes: Data Instrum Methods Agric Ind Med 2011;69(10):1546–53.
[27] Swarna M, Sowmya V, Soman KP. Effect of denoising on dimensionally reduced sparse hyperspectral unmixing. Procedia Comput Sci 2017;115:391–8.
[28] Xiong Peng, Wang Hongrui, Liu Ming, Zhou Suiping, Hou Zengguang, Liu Xiuling. ECG signal enhancement based on improved denoising auto-encoder. Eng Appl Artif Intell 2016;52:194–202.
[29] Huimin CUI, Ruimei ZHAO, Yanli HOU. Improved threshold denoising method based on wavelet transform. Phys Procedia 2012;33(1):1354–9.
[30] Han Xiaohong, Chang XiaoMing. An intelligent noise reduction method for chaotic signals based on genetic algorithms and lifting wavelet transforms. Inform Sci 2013;218:103–18.
[31] Ming-fu ZHAO, Ping TANG, Bin TANG, Peng HE, Yang-fei XU, Si-xing DENG, et al. Research on denoising of UV-Vis spectral data for water quality detection with compressed sensing theory based on wavelet transform. Spectrosc Spect Anal 2018;38(3):844–50.
[32] He Jian-Feng, Fang Fang, Yang Yao-Zong, He Yue-Shun, Tang Bin. Research on comparison and evaluation studies of several smoothing denoising method based on γ-ray spectrum detector. J Harbin Instrum Technol 2013;20(2):7–11.
[33] Yu-feng GUO. The disposal of gentle filter on natural gamma energy spectrum. J Daqing Petrol Instrum 2003;27(3):110–2.
[34] Huifen Li, Xiangqian Jiang, Zhu Li. Study and improvement of robust performance of gaussian filtering. Chinese J Sci Instrum 2004;25(5):633–7.
[35] Zai-yu DUAN, Jian-hua CHEN, Gui-xin ZHANG, Jun-jun GONG. Disposal of smooth γ spectrum on matlab process. Nucl Power Eng 2007;3(28):125–7.
[36] Meng-Hua ZHU, Liang-Gang LIU, Dong-Xu QI, Zhong YOU, Ao-Ao XU. Least square fitting of low resolution gamma ray spectra with cubic B-spline basis functions. Chin Phys C 2009;33(1):24–30.
[37] Jing-lun LI, Wu-yun XIAO, Xian-yun AI, Shan-qiang WANG. Convex optimization based total variation regularization smoothing for γ spectra. Nucl Electron Detect Technol 2018;1(38):111–6.
[38] Bianchia Davide, Lenauera Claudia, Betzb Gerhard, Vernes Andras. A wavelet filtering method for cumulative gamma spectroscopy used in wear measurements. Appl Radiat Isot 2017;120:51–9.
[39] Safari MJ, Abbasi Davani F, Afarideh H, Jamili S, Bayat E. Discrete fourier transform method for discrimination of digital scintillation pulses in mixed neutron-gamma fields. IEEE Trans Nucl Sci 2016;63(1):325–32.
[40] Minty B. Accurate noise reduction for airborne gamma—ray spectrometry. Explor Geophys 2003;34(3):207–15.
[41] Carè Algo, Garatti Simone, Campi Marco C. A coverage theory for least squares. J Roy Stat Soc 2017;79(5):1367–89.
[42] Hessari Peyman. Pseudo-spectral least squares method for linear elasticity. Comput Math Appl 2018;76(6):1356–71.
[43] Fujii Kazuyuki. Least squares method from the view point of deep learning. Adv Pure Math 2018;5:485–93.
[44] Belov A. A mathematical-statistics approach to the least squares method. Comput Math Model 2018;29(1):30–41.
[45] Sun Sida, Fang Sheng, Zhang Liguo, Li Hong, Tong Jiejuan, Jingyuan Qu. Improving the accuracy of gamma spectrum analysis by total variation based adaptive smoothing. International conference on nuclear engineering. 2013.
[46] Yang Xiaowei, Tan Liangjun, He Lifang. A robust least squares support vector machine for regression and classification with noise. Neurocomputing 2014;140:41–52.
[47] Qin WANG, Jian-feng HE, Yuan WANG, Hai-lin XIAO. The γ spectrum smoothing method and its evaluation with NaI(Tl) detector. Nucl Electron Detect. Technol 2015;35(1):13–7.
[48] Jun LIU, Xian GUAN, Feng YANG, Qing-ming HOU, Zhi-chao YANG, He-xi WU, et al. Airborne γ spectrum analysis based on LS-SVM segmented noise reduction method. Nucl Electron Detect Technol 2017;37(1):24–8.
[49] Xiao GANG, Deng LI, Zhang BENAI, Zhu JIANSHI. A Nonlinear wavelet method for data smoothing of low-level gamma-ray spectra. J Nucl Sci Technol 2004;41(1):73–6.
[50] Cairo. Fourier transformation methods in the field of gamma spectrometry. Pramana 2006;67(3):457–66.
[51] Siuda R, Engelhard H, Goldmann A, Cyrankiewicz M, Balcerowska G. PCA-based analysis of X-ray-excited Auger spectra from non-ordered Ag(110). Czech J Phys 2013;53(1):63–7.
[52] Yang Wu, Dong Yu, Jiang Jia, Li Haiqing, Zhu Tongming, Chen Shiyi. Evaluation of the Bone-ligament and tendon insertions based on Raman spectrum and its PCA and CLS analysis. Sci Rep 2017;7:1–6.
[53] Pinto Rui Climaco, Bosc Véronique, Noçairi H, Barros António S, Rutledge Douglas N. Using ANOVA-PCA for discriminant analysis: application to the study of mid-infrared spectra of carraghenan gels as a function of concentration and temperature. Anal Chim Acta 2018;629(1–2):47–55.
[54] Ledoit Olivier, Wolf Michael. Spectrum estimation: A unified framework for covariance matrix estimation and PCA in large dimensions. J Multivariate Anal 2015;139(C):360–84.
[55] Secmen M. Radar target classification method with high accuracy and decision speed performance using MUSIC spectrum vectors and PCA projection. Radio Sci 2016;46(5):1–9.
[56] Im Hee-Jung, Lee Yun-Hee, Park Yong Joon, Song Byoung Chul, Hwan Jung, Kim Won-Ho. Noise reduction in prompt gamma spectra acquired in short times. Nucl Instrum Methods Phys Res A 2007;574(2):272–9.
[57] Burr T, Hengartner N, Matzner-Lober E, Myers S, Rouviere L. Smoothing low resolution gamma spectra. IEEE Trans Nucl Sci 2010;57(5):2831–40.
[58] Zhang Jinzhao, Xiangguo Tuo. High-resolution gamma spectroscopy shift-invariant wavelet de-noising. Chin Phys C 2013.
[59] Li Huailiang, Tuo Xianguo, Shi Rui, Zhang Jinzhao, Henderson Mark Julian, Courtois Jérémie, Yan Minhao. A de-noising algorithm to improve SNR of segmented gamma scanner for spectrum analysis. Nucl Instrum Methods Phys Res Sect Accel Spectrometers Detectors Assoc Equipment 2016;818:68–75.
[60] Nick Kingsbury BY. Image processing with complex wavelets. Philos Trans Roy Soc B Biol Sci 1999.
[61] Jia YANG, Xiao-li LI. Denoising of ground gamma-ray spectra by NASVD method. Nucl Electron Detect Technol 2017;37(2):134–7.
[62] Zhu Meng-Hua. On estimating the background of remote sensing gamma-ray spectroscopic data. Nucl Instrum Methods Phys Res A 2016;832:259–63.
[63] Yiming Wang, Yixiang Wei. Baseline elimination method for γ-ray spectra based on improved SNIP algorithm. Nucl Electron Detect Technol 2012;32(12):1356–93.
[64] Tervo RJ, Kennett TJ, Prestwich WV. An automated background estimation procedure for gamma ray spectra. Nucl Instrum Methods 1983;216:205–18.
[65] Dermer Charles D. The extragalactic γ-ray background. First Glast Symp 2007;921:122–6.
[66] Lindstrom Richard M, Lindstrom David J, Slaback Lester A, Langland John K. A low-background gamma-ray assay laboratory for activation analysis. Nucl Instrum Methods Phys Res A 1990;299:425–9.
[67] Liyan Zhang, Chunlai Li, Jinazhon Liu, Yongliao Zou, Ziyuan OuYang. Background deduction of the Chang'E-1 gamma-ray Spectrometer data. Chin J Geochem 2012;31:234–41.
[68] Medhat ME, Wang Yifang. Estimation of background spectrum in a shielded HPGe detector using Monte Carlo simulations. Appl Radiat Isot 2014;84:13.

[69] Mishev AL, Hristova E. Recent gamma background measurements at high mountain altitude. J Environ Radioact 2012;113:77–82.
[70] Kneiske TM. Gamma-ray background: a review. Chin J Astron Astrophys 2007.
[71] Bogatov SA, Shvedov AM. Reconstruction of the background spectrum for processing airborne gamma survey data. At Energy 2011;111(1):48–54.
[72] Westmeier W. Background subtraction in Ge(Li) gamma-ray spectra. Nucl Instrum Methods 1981;180:205–10.
[73] Yin WM, Liu HZ, Tang B. Discussion and application of eliminating the background in γ-ray spectrum by SNIP algorithm. J East China Inst Technol 2009;32(3):245–8.
[74] Fornasa Mattia, Sánchez-Conde Miguel A. The nature of the diffuse gamma-ray background. Phys Rep 2015;598:1–58.
[75] Heusser G. Studies of y-ray background with a low level germanium spectrometer. Nucl Instrum Methods Phys Res B 1991;58(1):79–84.
[76] Najafi SI, Fedoroff M. Accurate gamma-ray spectrum analysis. J Radioanal Nucl Chem 1985;89(1):143–52.
[77] Alamaniotis Miltiadis, Heifetz Alexander, Raptis Apostolos C, Tsoukalas Lefteri H. Background spectrum estimation for low count spectra using kernel-modeled gaussian processes. Trans Am Nucl Soc 2012;106:273–4.
[78] Morháč Miroslav. Sophisticated algorithms of analysis of spectroscopic data. Proc Sci 2008;208.
[79] Mariscotti MA. A method for automatic identification of peaks in the presence of background and its application to spectrum analysis. Nucl Instrum Methods 1967;50(2):309–20.
[80] Statham PJ. A comparative study of techniques for quantitative analysis of the X-ray spectra obtained with a Si(Li) detector. X-ray Spectrum 1976;5:16–28.
[81] Gerasimov SA. Simple method for background subtraction in gamma-ray spectra. International Journal of Radiation Applications and Instrumentation. Part A Appl Radiat Isot 1992;43(12):1529–31.
[82] Morháč Miroslav, Kliman Ján, Matousek Vladislav. Background elimination methods for multidimensional coincidence γ-ray spectra. Nucl Instrum Methods Phys Res A 1997;401(1):113–32.
[83] Morháč Miroslav. An algorithm for determination of peak regions and baseline elimination in spectroscopic data. Nucl Instrum Methods Phys Res A 2009;600(2):478–87.
[84] Morháč Miroslav, Matousek Vladislav. Peak clipping algorithms for background estimation in spectroscopic data. Appl Spectrosc 2008;62(1):91–106.
[85] Long B, Feng TC, Su CY, Wu R, Pang L, Liu J. A self -adaptive method for the clipping of scatter background of γ spectrum. Nucl Electron Detect Technol 2013;33(10):1293–6.
[86] Shi Rui, Tuo Xianguo, Zheng Honglong, Yao Xiaoyu, Liu Yuqi, Shi Fanrong. Step-approximation SNIP background-elimination algorithm for HPGe gamma spectra. Nucl Inst Methods Phys Res A 2018;885:60–6.
[87] He Jianfeng, Xiao Hailing, Yang Yaozong, Jianhui Qu, Hongkun Xu, Lin Liu. A study of background subtraction method for NaI(Tl) instrument spectrum based on adaptive FWHM. Proceedings of the 3rd international conference on mechanical engineering and intelligent systems (ICMEIS 2015). 2015. p. 462–8.
[88] Hampton CV, Lian B, McHarris WmC. Fast-Fourier-transform spectral enhancement techniques for γ-ray spectroscopy. Nucl Inst Methods Phys Res A 1994;353(1–3):280–4.
[89] Zhang QX, Ge LQ, Gu Y, Lin YC, Zeng GQ, Yan J. Background estimation based on Fourier Transform in the energy-dispersive X-ray fluorescence analysis. X-Ray Spectrom 2012;41(2):75–9.
[90] Steenstrup S. A simple procedure for fitting a background to a certain class of measured spectra. J Appl Crystallogr 1981;14(8):226–9.
[91] Burgess Donald D, Tervo Richard J. Background estimation for Gamma-ray spectroscopy. Nucl Instrum Methods 1983;214:431–4.
[92] Clayton CG, Spackman R. Background reduction and signal enhancement for radioactive sources and radiation detectors in relative movement. Nucl Geophys 1987;1(1):25–40.
[93] MengHua Zhu, Liu LiangGang Xu, AoAo Ma Tao. Automatic estimation of peak regions in gamma-ray spectra measured by Nai detector. Chin Phys Lett 2008;25(11):3942–5.
[94] Goicoechea HC, Culzoni MJ, Gil Garcia MD. Chemometric strategies for enhancing the chromatographic methodologies with second-order data analysis of compounds when peaks are overlapped. Talanta 2011;83(4):1098–107.
[95] Michael A, Zhuo YN, Yavuz M, Khan MI. Deconvolution of overlapping peaks from differential scanning calorimetry analysis for multi-phase NiTi alloys. Thermochimica Acta 2018;665:53–9.
[96] Zheng Ying, Tian Di, Liu Ke, Bao Zemin, Wang Peizhi, Qiu Chunling, Liu Dunyi, Fan Runlong. Peak detection of TOF-SIMS using continuous wavelet transform and curve fitting. Int J Mass Spectrom 2018;428:43–8.
[97] Romanenko SV, Stromberg AG, Selivanova EV, Romanenko ES. Resolution of the overlapping peaks in the case of linear sweep anodic stripping voltammetry via curve fitting. Chemome Intell Lab Syst 2004;73(1):7–13.
[98] Larionova Ekaterina, Romanenko Serge. Determination of overlapping peaks heights by tangent method. 2012.
[99] Gardner Robin P, Ai Xian-yun, Peeples Cody R, Wang Jiaxin, Lee Kyoung, Peeples Johanna L, Calderon Adan. Use of an iterative convolution approach for qualitative and quantitative peak analysis in low resolution gamma-ray spectra. Nucl Instrum Methods Phys Res Sect A: Accel Spectrometers Detectors Assoc Equip 2011;652:544–9.
[100] Fernández-González A, Montejo-Bernardo JM. Natural logarithm derivative method: a novel and easy methodology for finding maximums in overlapping experimental peaks. Spectrochimica Acta Part A: Mol Biomol Spectrosc 2009;74(3):714–8.
[101] Fernández-González A, Montejo-Bernardo JM. Natural, logarithm derivative method: a novel and easy methodology for finding maximums in overlapping experimental peaks. Spectrochim Acta Part A 2009;74:714–8.
[102] Li Fei, Zhixing Gu, Ge Liangquan, Sun Di, Deng Xutao, Wang Shun, et al. Application of artificial neural networks to X-ray fluorescence spectrum analysis. X-Ray Spectrom 2018;48(2):138–50.
[103] Guo-yang YE, Ke-jun XU. Development of method and software for data processing in gas chromatograph. Acta Metrologica Sinca 2017;38(5):532–7.
[104] Fernández-González Alfonso, Montejo-Bernardo Jose Manuel. Natural logarithm derivative method: a novel and easy methodology for finding maximums in overlapping experimental peaks. Spectrochimica Acta Part A: Mol Biomol Spectrosc 2009;74(3):714–8.
[105] Wang Guowei, Yang Chunhua, Zhu Hongqiu, Li Yonggang, Peng Xiongwei, Gui Weihua. State-transition-algorithm-based resolution for overlapping linear sweep voltammetric peaks with high signal ratio. Chemometrics Intell Lab Syst 2016;151:61–70.
[106] Dubrovkin Joseph. Evaluation of undetectable perturbations of peak parameters estimated by the least square curve fitting of analytical signal consisting of overlapping peaks. Chemometrics Intell Lab Syst 2016;153:9–21.
[107] Dragan J, Mirta B, Rudolf S. On the existence of the nonlinear weighted least squares estimate for a three-parameter Weibull distribution. Comput Stat Data Anal 2008;52(9):4502–11.
[108] Hong-qiu ZHU, Guo-wei WANG, Chun-hua YANG, Yu CAO, Wei-hua GUI. Overlapped peaks resolution for linear sweep polarography using Gaussian-like distribution. Trans Nonferrous Met Soc China 2013;23(7):2181–6.
[109] Huang W, Henderson TLE, Bond AM, Oldham KB. Curve fitting to resolve overlapping voltammetric peaks: model and examples. Anal Chim Acta 2005;304(1):1–15.
[110] Zhi-MinZhang ShanChen, Liang Yi-Zeng. Peak alignment using wavelet pattern matching and differential evolution. Talanta 2011;83(4):1108–17.
[111] Bappa Mukherjee V, Srivardhan PNS Roy. Identification of formation interfaces by using wavelet and Fourier transforms. J Appl Geophys 2016;128:140–9.
[112] Palencia Manuel. Functional transformation of Fourier-transform mid-infrared spectrum for improving spectral specificity by simple algorithm based on wavelet-like functions. J Adv Res 2018;14:53–62.
[113] Liu Tao, Li Jian, Cai Xiaofeng, Yan Shaoze. A time-frequency analysis algorithm for ultrasonic waves generating from a debonding defect by using empirical oust transform. Appl Acoust 2018;131:16–27.
[114] Strain John. Fast Fourier transforms of piecewise polynomials. J Comput Phys 2018;373:346–69.
[115] Fletcher P, Sangwine SJ. The development of the quaternion wavelet transform. Signal Process 2017;136:2–15.
[116] Zheng Jinde, Pan Haiyang, Yang Shubao, Cheng Junsheng. Adaptive parameter-less empirical wavelet transform based time-frequency analysis method and its application to rotor rubbing fault diagnosis. Signal Process 2017;130:305–14.
[117] Peng ZK, Tse Peter W, Chu FL. A comparison study of improved Hilbert-Huang transform and wavelet transform: application to fault diagnosis for rolling bearing. Mech Syst Sig Process 2005;19:974–88.
[118] Li Yuan-lu, Tang Hui-qiang, Chen Hai-xiu. Fractional-order derivative spectroscopy for resolving simulated overlapped Lorenztian peaks. Chemometrics Intell Lab Syst 2011;107(1):83–9.
[119] Zheng Ying, Fan Runlong, Qiu Chunling, Liu Zhen, Tian Di. An improved algorithm for peak detection in mass spectra based on continuous wavelet transform. Int J Mass Spectrom 2016;409:53–8.
[120] Jiao Long, Gao Suya, Zhang Fang, Li Hua. Quantification of components in overlapping peaks from capillary electrophoresis by using continues wavelet transform method. Talanta 2008;75(4):1061–7.